SCIENTIFIC REPORTS

OPEN

SUBJECT AREAS:
RECEPTORS
DEVELOPMENT
SYNAPTIC TRANSMISSION
PLASTICITY

Received
18 January 2012

Accepted
20 February 2012

Published
12 March 2012

Correspondence and requests for materials should be addressed to S.E.L (sari.lauri@helsinki.fi)

Expression of GluK1c underlies the developmental switch in presynaptic kainate receptor function

Aino Vesikansa[1,2], Prasanna Sakha[1,2], Juha Kuja-Panula[1], Svetlana Molchanova[1,2], Claudio Rivera[1,3], Henri J. Huttunen[1], Heikki Rauvala[1], Tomi Taira[1,4] & Sari E. Lauri[1,2]

[1]Neuroscience Center, University of Helsinki, Finland, [2]Department of Biosciences, Physiology, University of Helsinki, Finland, [3]Université de la Méditerranée, UMR S901 Aix-Marseille 2, INMED (Institut de Neurobiologie de la Méditerranée), Marseille, 13009, France, [4]Department of Veterinary Biosciences, University of Helsinki, Finland.

Kainate-type glutamate receptors (KARs) regulate synaptic transmission and neuronal excitability via multiple mechanisms, depending on their subunit composition. Presynaptic KARs tonically depress glutamatergic transmission during restricted period of synapse development; however, the molecular basis behind this effect is unknown. Here, we show that the developmental and cell-type specific expression pattern of a KAR subunit splice variant, GluK1c, corresponds to the immature-type KAR activity in the hippocampus. GluK1c localizes to dendritic contact sites at distal axons, the distal targeting being promoted by heteromerization with the subunit GluK4. Presynaptic expression of GluK1c strongly suppresses glutamatergic transmission in cell-pairs *in vitro* and mimics the immature-type KAR activity at CA3-CA1 synapses *in vivo*, at a developmental stage when the endogenous expression is already downregulated. These data support a central role for GluK1c in mediating tonic inhibition of glutamate release and the consequent effects on excitability and activity-dependent fine-tuning of the developing hippocampal circuitry.

Kainate-type of glutamate receptors (KARs) consist of homo- or heteromeric combinations of five subunits (GluK1-5; previously known as GluR5-7, KA1 and KA2;[1]) and act as key modulators of neuronal function in several areas of the brain. The precise role of KARs is strictly dependent on their subcellular localization and subunit composition that varies between cell types and during development. At the presynaptic compartment, KARs regulate transmitter release at both glutamatergic and GABAergic synapses and control presynaptic forms of short-and long-term synaptic plasticity[2–4]. In the neonate CA1, presynaptic KARs are tonically activated by ambient glutamate, causing continuous physiological suppression of glutamate release[5]. In addition to the physiological relevance in controlling information transfer at the developing hippocampal circuitry, tonic KAR activity is critical for formation and maturation of CA3-CA1 glutamatergic synapses[6]. The immature-type KARs are gradually lost during second postnatal week in parallel with the activity-dependent maturation of the neuronal circuitry, and are replaced with adult – type KARs lacking tonic activity and with distinct downstream signaling mechanisms[5,7,8].

Many of the functions ascribed for KARs at developing glutamatergic synapses are sensitive to GluK1-subunit specific agonists and antagonists[5–9]. The molecular composition of these receptors could be diverse since these pharmacological tools act on both homomeric and heteromeric receptors containing the GluK1 subunit[10]. In addition, GluK1 subunits exist as three C-terminal splice variants (named GluK1a, GluK1b and GluK1c), which differ in their tissue-specific expression pattern, membrane delivery and protein interactions[11,12]. Heteromerization of GluK1 with the subunits GluK4-5 provides KARs with higher agonist affinity[13–15], necessary for activation by physiological concentrations of glutamate in the immature brain[5]. However, the cell-type specific expression profile or the developmental regulation of various GluK1 splice variants, as homomeric receptors or as heteromeric combinations with other KAR subunits is not known.

Here we show that in the developing hippocampus, the splice variants GluK1b and GluK1c are preferentially expressed in interneurons and pyramidal cells, respectively. GluK1c strongly co-localizes with the high-affinity subunit GluK4, which promotes its targeting to distal neuronal processes. We further demonstrate that expression of GluK1c at CA3 pyramidal neurons is sufficient to mimic the immature-type KAR activity at a developmental stage when the endogenous expression is already lost. These findings strongly suggest that the tonic

KAR activity inhibiting glutamate release in the neonate is due to developmentally restricted expression of GluK1c splice variant in the principal neurons.

Results

GluK1 mRNA is expressed in the principal neurons in the neonate hippocampus. *In situ* hybridization studies have demonstrated that GluK1 mRNA is prominently expressed in GABAergic interneurons at juveline/adult hippocampus[16–18]. However, functional data as well as some of the studies on GluK1 mRNA expression suggest that GluK1 is present also on hippocampal principal neurons during early postnatal development[5,9,19,20]. To determine the detailed expression pattern of GluK1 in different cell types (pyramidal vs. interneurons) during postnatal development, we performed double *in situ* hybridization experiments at P3 and P15 hippocampus. Probe against CaMKII-β isoform, highly expressed already early in development[21,22], was used as a marker for principal neurons. All S^{35}-labeled probes were first tested to ensure specific staining with anti-sense probe and to control that there was no unspecific signal with the corresponding sense mRNA (Supplementary Figure 1a,b).

At P3, GluK1 transcript was detected in CaMKII-β positive neurons (referred to as principal/pyramidal neurons or dentate granule cells from here on) everywhere in the hippocampus (Figure 1a,b). The expression of GluK1 declined strongly during development and at P15, co-expression of CaMKII-β and GluK1 was only observed in the dentate gyrus (Figure 1a,b). The distribution of GluK1 transcript between principal neurons and other cells in different regions of the hippocampus was estimated by calculating the percentage of double

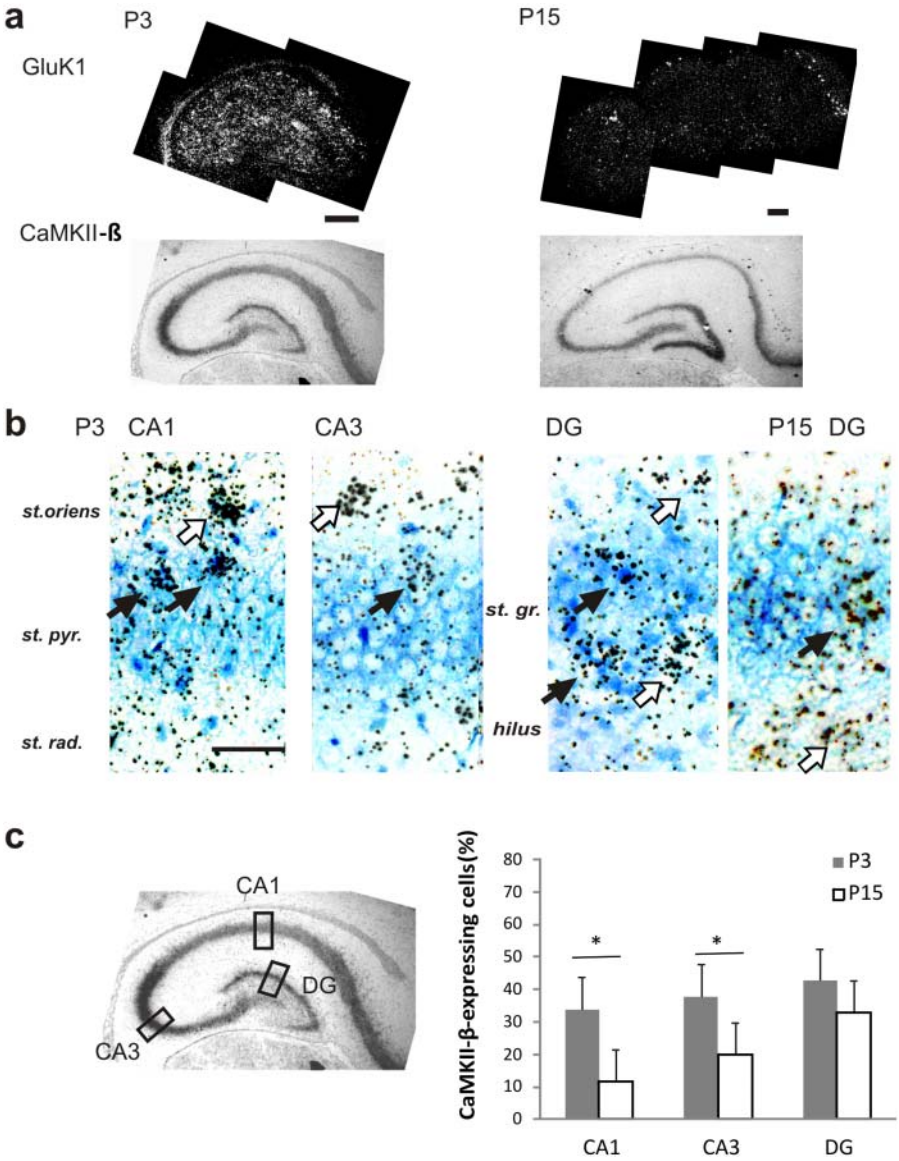

Figure 1 | Developmental regulation of GluK1 mRNA expression in the principal neurons of the hippocampus. (a) Images from i*n situ* hybridization with anti-sense GluK1 (S^{35}-labeled, dark field image) and CaMKII-β (dig labeled, bright field image) probes in P3 and P15 hippocampus. Scale bar 200 μm. (b) Higher magnification figures of the double *in situ* hybridization staining in the pyramidal layer of CA1, CA3 and in the granule cells of dentate gyrus (DG). GluK1 staining is observed as black granules, superimposed on the blue CaMKII-β staining at the bright field image. GluK1 expression is detected in both CaMKII-β positive (principal) neurons and CaMKII-β negative (inter-) neurons in all areas of the neonate hippocampus (black and white arrows, respectively), and in the granule cells at P15. Scale 50 μm. (c) Quantified data showing the distribution of GluK1 in principal neurons *vs* other cells in different areas of hippocampus. The values represent the percentage principal neurons (i.e. GluK1 + CaMKII-β positive cells) of all GluK1-expressing cells that were calculated in rectangular fields positioned as depicted on the left. The percentages were obtained by analysis of at least four independent sections, with a total of 40–64 cells in each group. All the error bars depict s.e.m. * $p<0.05$ with ANOVA on the raw data.

(i.e. CaMKII-β and GluK1) positive neurons of all GluK1 positive cells. The analysis was done within fixed size (0.1125 μm^2) rectangular regions as illustrated in the Figure 1c. At P3, 30–40 % of the cells expressing GluK1 were principal neurons in all areas studied (a total of 40–51 cells from 6–7 sections analyzed for each group, Figure 1c). This percentage was significantly reduced during the first two weeks of development in CA1 and in CA3 (11 % and 20 % at P15, respectively), but not in the dentate gyrus (n=46–64, Figure 1c). Thus, in the neonate hippocampus, GluK1 mRNA is expressed in both principal neurons and interneurons. During development, the expression in the pyramidal neurons is lost, resulting predominant expression of GluK1 in interneurons as well as dentate granule cells.

GluK1 is co-expressed with the high-affinity subunits GluK4 and GluK5 during early development. Functional studies suggest that the developmental switch in GluK1 containing KAR function is associated with the change in the affinity of receptors[5]. A possible mechanism for that is a change in heteromeric subunit composition of the receptors, in particular with high-affinity subunits GluK4 and/or GluK5. To examine possible alterations in the expression of GluK1 with GluK4 and GluK5 during development, we next analyzed the co-expression of these subunits by double *in situ* hybridization.

At P3, GluK4 was detected in principal cells layers of the areas CA1, CA3 and dentate gyrus (Figure 2a). Approximately 60% of the cells expressing GluK1 were also positive for GluK4 in these areas (n=49–65; Figure 2b,c). In the juvenile (P15), GluK4 was not detected in CA1 area, but was mainly expressed in CA3 pyramidal cells layer and in some granule cells, as reported previously[18,23]. The co-expression of GluK1 and GluK4 decreased significantly during development, and at P15 few cells expressing GluK1 and GluK4 were detected in area CA3, while some co-expression (26%) remained in the dentate gyrus (n=38–64; Figure 2c).

GluK5 was expressed in all pyramidal cell layers at P3 (Figure 2a). As seen with GluK4, GluK1 was co-expressed with GluK5 at P3 in all areas studied, though in a lesser degree: co-expression was detected in 30–40% of GluK1 positive cells (n=36–40; Figure 2b,d). Similarly, the co-expression of GluK1 and GluK5 decreased considerable during the second postnatal week in areas CA1 and CA3 while no change was seen in the dentate gyrus (n=41–47; Figure 2d). Together, this data indicates that in the neonate, GluK1 is expressed in the same cells as the high-affinity subunits GluK4 and GluK5, and co-expression is strongly reduced during development. This is mainly due to the loss of GluK1 expression in pyramidal neurons.

GluK1c is the predominant splice variant expressed in the pyramidal neurons. To study the expression profile of GluK1 splice variants in the neonate hippocampus, we first performed RT-PCR experiments from two time points (P3 and P15). In line

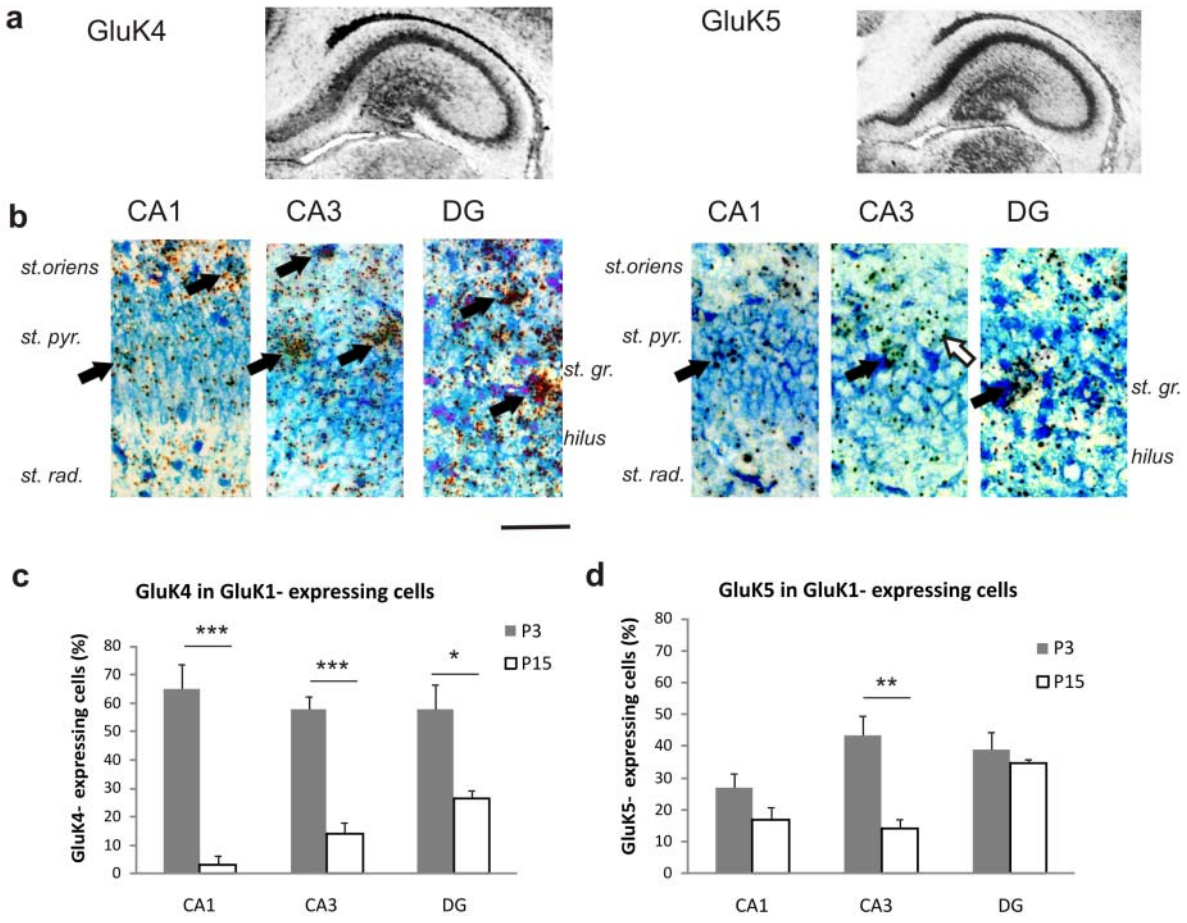

Figure 2 | GluK1 is co-expressed with the high-affinity subunits GluK4 and GluK5 in the neonate hippocampus. (a) *In situ* hybridization for GluK4 and GluK5 mRNA in P3 hippocampal sections. Both subunits are widely expressed in principal neurons of the hippocampus during early postnatal development. (b) Double *in situ* hybridization for GluK1 (S^{35}) and GluK4/GluK5 (dig) in areas CA1, CA3 and in the dentate gyrus (DG) at P3. At P3, GluK1 and GluK4 are strongly co-localized in all regions of the hippocampus (black arrows), while co-expression of GluK1 and GluK5 is strongest in the area CA3. White arrows: GluK1 positive but GluK4/5 negative neurons. Scale 50 μm. (c,d) Quantification of the GluK1-GluK4/5 co-expression at different hippocampal subfields at P3 vs P15. The values represent the percentage of GluK1 and GluK4/GluK5 double positive cells of all GluK1 positive cells. 38–65 neurons from at least four sections were analyzed for each group. All the error bars depict s.e.m. * $p<0.05$, ** $p<0.01$, ***$p<0.005$ with ANOVA on the raw data.

with the previous results[11], GluK1a was not detected in the hippocampus neither at P3 or P15, while GluK1b and -c were expressed at both developmental stages (Figure 3a). This allowed us to focus on GluK1b and -c variants in the following experiments.

The developmental decrease in GluK1 expression in pyramidal neurons may be a consequence of the down-regulation of either GluK1b or GluK1c mRNA or both. To distinguish between these possibilities, we designed an oligodeoxyribonucleotide probe against the c-terminal sequence encoding for the 29 amino acid insert present in the c-splice variant but not in GluK1a or -b. In parallel, a probe of approximately same length against the insert flanking regions was used (Supplementary Figure 1c). The specificity of these probes against GluK1 b and –c splice variants was first tested using dot – blot assay. The probe against the GluK1c sequence showed no cross – reactivity with GluK1b, while the other probe recognized both the GluK1b- and c splice variants (Supplementary Figure 1d).

In situ hybridization with the radioactively labeled GluK1c and GluK1b/c probes produced a patterned signal in the neonate (P3) hippocampus (Figure 3b), while the corresponding sense-probes had no reactivity (Supplementary Figure 1e). Further, the staining pattern of the GluK1b/c probe was very similar to that obtained with the long (503 bp) GluK1 – specific probe (Figure 1), further suggesting that the short probes (99 and 87 bp) worked in a specific manner under our hybridization conditions. In parallel *in situ* hybridizations from P15 rat brain sections, the expression level of both GluK1b/c and GluK1c transcripts in the hippocampus was considerably lower than at P3. Quantification of the x-ray films exposed to sections hybridized with the different radioactive probes indicated that the expression of splice variant GluK1c decreased significantly more during development as compared to the signal obtained with GluK1b/c probe (Figure 3d; n=4 sections for each group; $p<0.04$).

To examine whether the splice variants differ in their expression pattern, we performed double *in situ* hybridization with CaMKII-β. Interestingly, while the signal obtained with the GluK1b/c probe was predominantly localized in the non-pyramidal neurons as expected, the splice variant GluK1c was preferentially detected at pyramidal neurons at P3, particularly in the area CA3 (n=66–127; Figure 3c,e). The splice variants distributed equally between principal and non-principal neurons in the dentate gyrus.

These results suggest that GluK1b and GluK1c differ in their cell-type specific expression patterns as well as in their developmental regulation. At P3, the expression of GluK1 in pyramidal cells can be fully explained by the expression of the GluK1c splice variant. During development, the expression of GluK1c decreases significantly, and as a consequence the expression of GluK1 in the pyramidal neurons is lost.

Subcellular targeting of GluK1c in dispersed cultures of hippocampal neurons is regulated by GluK4 and GluK5 subunits. The *in situ* - data shows that GluK1c is the main splice variant

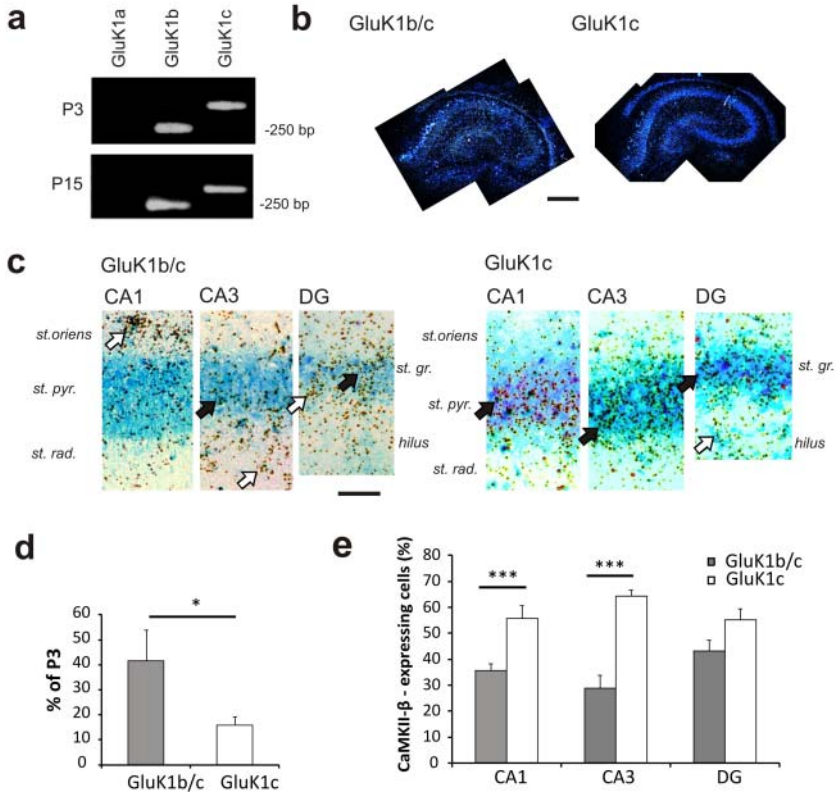

Figure 3 | GluK1b and GluK1c splice variants are preferentially expressed in principal neurons and interneurons of the neonate hippocampus, respectively. (a) RT-PCR results illustrating expression of GluK1b and -c splice variants in the neonatal and juvenile hippocampus. GluK1a was not detected in the hippocampus at either developmental stage. (b) Dark field *in situ* hybridization images showing the GluK1b and -c (S^{35}) mRNA expression in the neonate (P3) hippocampus. Scale 200 µm. (c) Double *in situ* hybridization for GluK1b/c (S^{35}) and CaMKII-β (dig) in areas CA1, CA3 and in dentate gyrus (DG) at P3. GluK1b/c staining is mainly detected in CaMKII-β negative cells (white arrows) while GluK1c staining strongly colocalizes with CaMKII-β in the principal neurons (Black arrows). Scale 50 µm. (d) Quantified data on the developmental regulation of the GluK1b/c mRNA expression in the hippocampus. Values represent the percentage of the GluK1 mRNA expression at P15 as compared to the level at P3, analyzed from x-ray films exposed to sections from parallel *in situ* hybridizations at the two developmental stages. Both splice variants are strongly downregulated during development. (e) Quantified data on the distribution of GluK1b/c and c splice variants in pyramidal neurons *vs.* interneurons in different areas of hippocampus. The values represent the percentage of pyramidal neurons (i.e. double positive cells) of all GluK1-expressing cells at P3. 66–127 neurons from at least 4 sections were analyzed for each group. All the error bars depict s.e.m. *** $p<0.005$ with ANOVA on the raw data.

expressed in pyramidal neurons in the neonate hippocampus and suggest that GluK1c, probably as heteromeric receptor with GluK4/5, is responsible for the tonic presynaptic KAR activity early in development. However, it is not known whether these receptors can localize to axonal compartment in hippocampal neurons. Since the lack of specific antibodies for GluK1 prevents analysis of subcellular localization of the endogenous protein, we produced epitope tagged constructs for GluK1c, GluK4 and GluK5 in lentiviral vector under synapsin-1 promoter to drive neuron specific expression. By lentiviral expression we were able to screen a high number of neurons as the transduction efficiency in dispersed hippocampal neurons was close to 100%.

The subcellular localization pattern of flag-tagged GluK1c was divided into two groups; neurons in which GluK1 was detected only in soma and proximal dendrites (restricted to soma-group) and neurons in which GluK1 was also detected in distal dendritic processes (distal dendrites-group). In addition, axonal localization was analyzed by identifying flag-stained neuronal processes lacking MAP2-immunostaining. When expressed alone, GluK1c was mainly restricted to soma and proximal dendrites (61% of neurons, n=245) (Figure 4a,b), and GluK1c staining in axons was only detected in a subset of neurons expressing GluK1 in distal dendrites (5% of all neurons, 11% of neurons expressing GluK1c in distal dendrites; n = 245).

Localization of GluK1a splice variant within the dendritic compartment has been shown to depend on GluK2 and GluK5[24]. To study whether the high-affinity subunits were able to change the subcellular targeting of GluK1c splice variant, it was co-expressed with either GluK4 or GluK5 in hippocampal neurons. Co-expression of both GluK4 and GluK5 clearly increased the proportion of cells where GluK1c splice variant was detected in the distal dendrites (171% and 176%, of the level with GluK1c alone, respectively; n=336 and n=167; Figure 4a,c). The axonal localization of GluK1c was apparently enhanced upon GluK4 co-expression (152%), although this effect did not reach statistical significance. In contrast, co-expression of GluK5 significantly reduced the fraction of cells in which GluK1c was detected in axons (10%).

GluK1c localizes to dendritic contact sites at distal axons. Weak expression in the axonal processes is difficult to observe in a dispersed cell culture, thus complicating the analysis of GluK1 axonal localization. To overcome this problem, we cultured hippocampal neurons in compartmentalized chambers[25]. These microfluidic culture platforms contain small tunnels where axons, due to their faster growth rate, grow in isolation[25], thus allowing their high-resolution imaging without dendritic of somatic contamination. Since glial cells no not invade the tunnels in these culture platforms, we were able to further enhance the resolution of analysis by expressing the KAR subunits under strong but not neuron specific CMV promoter. As shown before, dendritic growth was only observed in the initial part of the tunnel, and no MAP2 positive processes were detected > 300 μm from the tunnel opening (Figure 5a; 25,26). Analysis GluK1c expressing neurons indicated that this subunit was indeed localized in the distal axons (59% of the axons in the middle section of the tunnels, n=136; Figure 5 a,b,d). Rate of lentiviral transduction was estimated by parallel pLen-Syn1/GFP infection, and was 70% (n=68). Co-expression of GluK4 did not change the percentage of GluK1c positive axons (58%, n=143) in contrast to co-expression of GluK5, which reduced axonal localization of GluK1c (38%, n=75; p=0,013 as compared to GluK1c alone; Figure 5c,d). On the other hand, the axonal localization of GluK4 but not GluK5 was slightly

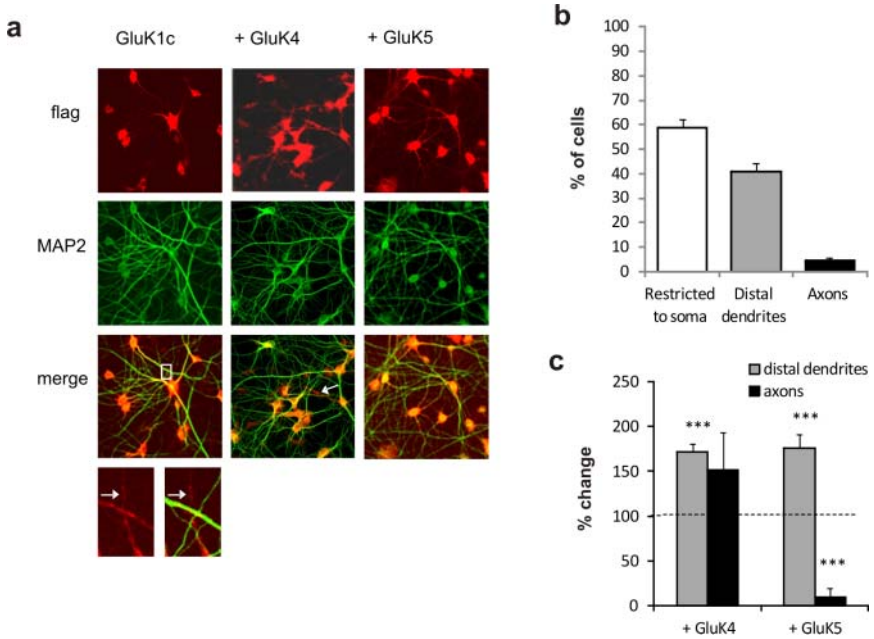

Figure 4 | Heteromerization with GluK4 and GluK5 promotes distal targeting of GluK1c in cultured hippocampal neurons. (a) Confocal images from cultured hippocampal neurons transduced with flag-GluK1c alone or together with myc-GluK4/5. Cells were stained with anti-flag (red) and anti-MAP2 (green) antibodies to visualize GluK1 and dendritic processes, respectively. GluK1c staining in MAP-negative (axonal) processes is indicated by arrows. (b) Quantified data on subcellular localization of GluK1c splice variant. The neurons were divided in groups where GluK1 was either restricted to soma or also localized in distal dendrites. The axons-group represent neurons with flag(GluK1) – stained, MAP2-negative processes. The data represents the percentage of cells in each group and analysis of 245 neurons from 3 independent stainings. (c) The effect of GluK4 and GluK5 co-expression on subcellular localization of GluK1c. GluK4 co-expression enhanced localization of GluK1c in distal dendrites, while there was no significant effect on its axonal targeting. GluK5 co-expression promoted dendritic localization of GluK1c with associated reduction in axonal staining. The data represents analysis of 167–336 neurons from at least 3 independent stainings, and has been normalized to the data shown in b, (i.e. no change in localization as compared to expression of GluK1c alone = 100%). All the error bars depict s.e.m. *** $p<0.005$ with ANOVA on the raw data.

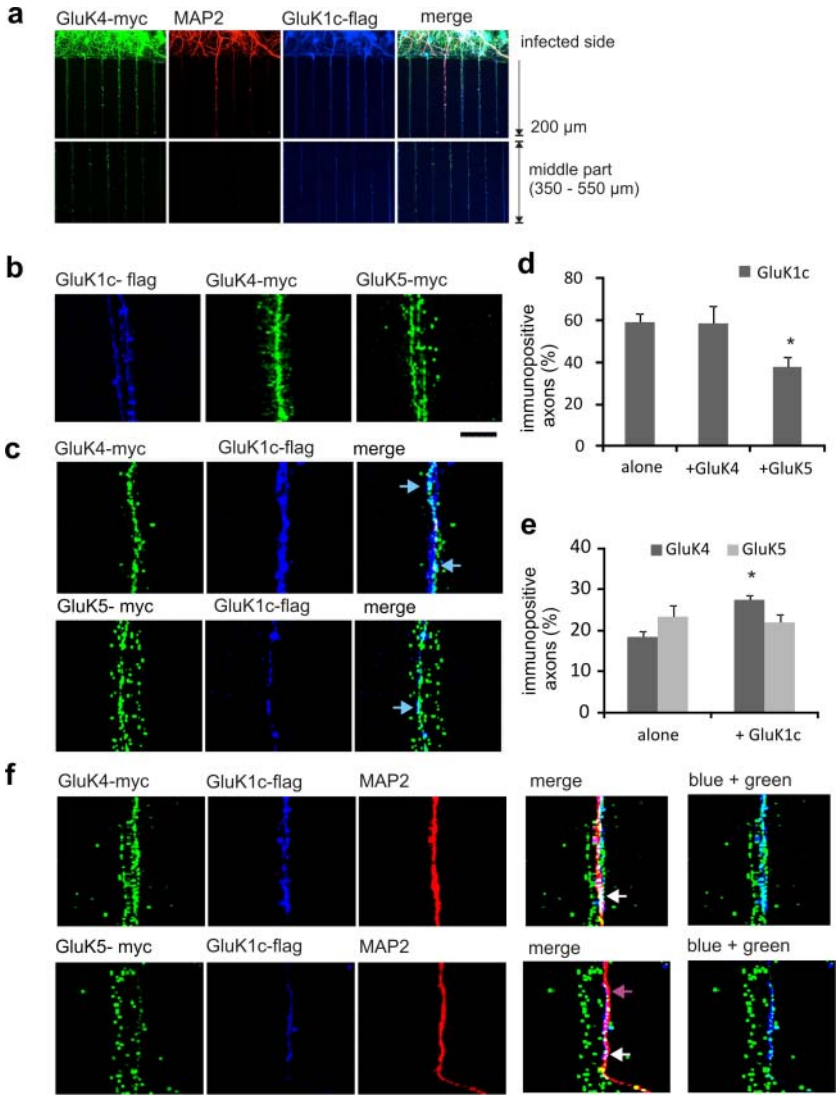

Figure 5 | High-resolution analysis of axonal GluK1c using microfluidic hippocampal cultures. (a) Confocal image showing an example of lentivirally infected hippocampal neurons grown in a compartmentalized (microfluidic) culture. The culture platform has small tunnels extending from the main reservoir (top), that allow entry of neurites but not cell bodies. MAP2 immunostaining (red) illustrates growth of dendritic processes only in the initial part of the tunnel (< 300 µm from tunnel opening) but not in the middle (lower panels). anti-myc (green) and anti – flag (blue) immunostaining was used to visualize lentivirally expressed GluK4-myc and GluK1c – flag in the axons. Scale 7 µm (for all panels in b,c,f).(b) A high-magnification figures from the mid-part of the tunnels, illustrating expression of GluK1c –flag, GluK4-myc and GluK5-myc in axonal shaft and protrusions. (c) Co-expression of GluK1c-flag with GluK4-myc (top) or GluK5-myc (lower panel). Co-localization (arrows) in isolated axons was observed mainly in the axon body and only in a subset of axonal protrusions. (d) Quantified data on axonal localization of GluK1c. The values represent percentage of immunopositive axons from all detected axons (n=75–144/group), calculated from confocal and bright field images from the middle section of the tunnel, respectively. Axonal localization of GluK1c was slightly reduced upon GluK5 but not GluK4 co-expression. * $p<0.05$ with ANOVA on the raw data. (e) Similar data as in d, for axonal localization of GluK4 and GluK5 when expressed alone or together with GluK1c. Co-expression of GluK1c enhanced detection of GluK4 in axons. (f) Confocal pictures from the end of the tunnels, illustrating localization of GluK1c-flag co-expressed with GluK4-myc (top) or GluK5-myc (lower panel). The infected axons crawl on non-infected dendrites (red, MAP2 staining) that enter the tunnels from the other side of the chamber. Merged images show axonal GluK1c staining in the dendritic contact site (arrows), where it co-localizes with GluK4 and, to lesser extent with GluK5.

increased when GluK1c was co-expressed (Figure 5e). These data confirm that GluK1c as well as the high-affinity subunits GluK4 and GluK5 are targeted to the distal axons and are appropriately localized to regulate transmitter release.

Interestingly, high magnification images illustrated that while all of the subunits were detected both in the axonal shaft as well as in filopodial protrusions, GluK1c co-localized with GluK4 and GluK5 only in a subset of the immunostained axonal structures (Figure 5c). While GluK4 and in particular, GluK5 were most prominently detected at the axonal protrusions, GluK1c was preferentially localized to the axon shaft. The axons in the middle of the tunnels lack dendritic contacts, and the protrusions likely represent immature structures looking for postsynaptic target. At the end of the tunnels, however, axons contact dendrites from the non-infected side of the chamber. In this part, GluK1c was clearly localized at the dendritic contact site together with GluK4, while there was less co-localization of GluK1c with GluK5 (Figure 5f).

Presynaptic expression of GluK1c leads to robust inhibition of synaptic transmission in CA3-CA3 neuron pairs. The expression pattern and subcellular localization of GluK1 splice variants support the hypothesis that presynaptic functions of kainate receptors

during early development are mediated by GluK1c containing KARs. To directly test whether presynaptic expression of GluK1c is able to regulate synaptic transmission, CA3 pyramidal neurons in organotypic hippocampal cultures were infected with double-promoter lentiviral vectors containing GluK1c and EGFP under separate synapsin – 1 promoters (GluK1c_EGFP). Control slices were infected with a similar construct containing the GluK1b splice variant. It should be noted that the CA3 pyramidal neurons endogenously express GluK2, GluK4 and GluK5 KAR subunits to promote surface expression and distal targeting of GluK1 (e.g. 18, 11, 24).

Whole cell recordings were made from cell pairs, one of which was EGFP positive (i.e. lentivirally transduced). Depolarization induced action-potential firing in the transduced neuron induced post-synaptic glutamatergic current (EPSCs) in 20–30% of the recorded cell pairs (29% (n=34) and 20% (n=60) for control and GluK1c, respectively). The percentage of synaptically connected neurons in infected slices was slightly lower as compared to wild-type (non-infected) slices (40% (n=40)). Analysis of the EPSCs indicated that expression of GluK1c in the presynaptic neuron significantly reduced the success rate of EPSCs (Figure 6a,b,e). The mean amplitude of the successful EPSCs (potency) was slightly but not significantly reduced (Figure 6f). Further, paired pulse facilitation was higher in cell pairs expressing GluK1c presynaptically as compared to controls (Figure 6c,d,g). Together, these data indicate that presynaptic expression of GluK1c strongly reduces glutamate release probability.

To test whether the altered presynaptic function in GluK1 expressing neurons is due to ongoing tonic inhibition of glutamate release by presynaptic KAR, we applied ACET (100 nM), a selective antagonist of GluK1 subunit containing KARs[27]. In control neurons, ACET had no significant effect on EPSCs although a small run-down of the success rate was observed (Figure 6h). In neuron pairs where GluK1c was expressed presynaptically, ACET application increased the success rate to 138 ± 13% of control with no associated changes in potency (n=4). ACET was not able to enhance transmission efficacy to control levels, suggesting that GluK1c overexpression also resulted in enduring changes in the synaptic machinery that were independent on ongoing KAR activity.

Expression of GluK1c at juvenile CA3 mimics the immature-type KAR activity at CA3-CA1 synapses. The data from organotypic cultures indicate that expression of GluK1c at the presynaptic neuron can significantly inhibit glutamatergic transmission and thus mimic the tonic KAR activity that is observed at immature CA3-CA1 synapses. To study whether expression of recombinant GluK1c can recapitulate the immature type KAR activity at developmental stage when it is no longer endogenously expressed in the CA3, we used the lentiviral vectors (control (EGFP), GluK1c_EGFP) to infect CA3 area of neonatal (P0-P2) rat pups. Patch clamp recordings were made from CA1 pyramidal neurons in acute slices at P14-P15. Only slices where a strong fluorescence signal was detected selectively in area CA3 were used for experiments (Figure 7a).

The tonic KAR mediated inhibition at immature synapses is typically observed as smaller EPSC amplitude as well as an increase in the facilitation of EPSCs in response to short high-frequency stimulation[5]. Infection with the control virus had no significant effect on the EPSCs evoked by 5 pulses at 50 Hz as compared to non-infected animals (not shown). In contrast, expression of GluK1c caused significant inhibition of the amplitude of the first EPSC to a fixed test pulse as well as an increase in the facilitation of the following EPSCs during the 5 pulse 50 Hz stimulation (Figure 7b–d). We ensured pharmacologically that this effect was in fact due to GluK1 activity. In GluK1c infected animals, EPSC amplitude was increased to 303 ± 76% and the facilitation ratio decreased to 55 ± 4% of the baseline level in the presence of ACET (100 nM)(n=5; Figure 7e). These data strongly suggest that GluK1c splice variant inhibits glutamate release and is responsible for the tonic inhibition of transmission at immature CA3-CA1 synapses.

Discussion

Ionotropic glutamate receptor subunits undergo extensive post-transcriptional and post-translational modifications that may directly reflect their physiological role, by controlling biophysical properties, subcellular targeting and intracellular signaling of the receptors. However, very little is known about regulation and physiological functions of KAR splice variants. Here we show that developmentally restricted expression of GluK1c in the pyramidal neurons of the neonate hippocampus underlies tonic inhibition of glutamate release at immature synapses.

The expression of all the KAR subunits is regulated to some extent during development[18,19]. The mRNA of the GluK1c splice variant showed a particularly pronounced developmental regulation, being detected mainly (but not exclusively) in the pyramidal neurons and dentate granule cells during early postnatal development, after which a low level of expression was confined to the granule cells. During the first postnatal weeks, the granule cell population is developmentally heterogeneous[28], with new progenitors being generated until adulthood. Thus, it is possible that similar to pyramidal neurons, the expression of GluK1c in the granule cells is associated with a certain phase of maturation; these cells could be detected at various ages due to ongoing development of the region.

Intriguingly, the expression pattern of GluK1c corresponds well to the existing pharmacological data on endogenous GluK1 KARs regulating glutamate release. The developmentally restricted expression at the pyramidal neurons parallels the immature-type tonic KAR activity at the CA3-CA1 and CA3-CA3 synapses[5,9], while the expression in the granule cells supports the role of presynaptic GluK1 in the frequency-dependent regulation of transmission at the mossy fibre synapse (e.g. [29]). Finally, in addition to the effects on glutamatergic transmission, high-affinity GluK1 containing KARs have been shown to tonically inhibit GABA release from immature mossy fibre terminals[30]; an effect which could manifest the GluK1c expression in the neonate granule cells. On the other hand, expression of the GluK1b in the non-principal neurons throughout the early postnatal development suggests that this splice variant is mainly responsible for the functions attributed to GluK1 containing KARs in the GABAergic interneurons in the neonate hippocampus[31,32].

Since the immature-type KARs regulating glutamate release have a high agonist affinity, they likely contain either the subunit GluK4 or GluK5 in addition to GluK1c[5]. Furthermore, it has been suggested that heteromeric KARs possess binding and desensitization characteristics that can be localized to the particular subunit subtypes[33,15]. In particular, expression of GluK4/5 subunits confer a high-affinity, non-desensitizing agonist binding site[15] that may well underlie tonic KAR activity in the immature neurons. Data from GluK4 $^{-/-}$ and GluK4 $^{-/-}$/GluK5$^{-/-}$ animals suggest that these subunits are also critical for localizing KARs at both pre and postsynaptic sites[34]. While GluK5 has been reported to target GluK1a to distal dendrites[24], no previous data exists regarding the subcellular targeting of heteromeric GluK1c -GluK4/5 receptors. Our data confirms that GluK1c is localized in both distal dendrites as well as in axons of hippocampal neurons. Interestingly, co-expression of either of the high-affinity subunits GluK4 and GluK5 hippocampal neurons promoted localization of GluK1c at distal dendrites. In contrast to GluK4, however, GluK5 co-expression appeared to specifically promote polarized targeting of GluK1c to dendritic compartment, with associated reduction of GluK1c in axons. High-resolution images of recombinant GluK1c in isolated axons show that this subunit is localized to both, the axon body and axonal protrusions, where it partially co-localizes with the co-expressed high-affinity subunits

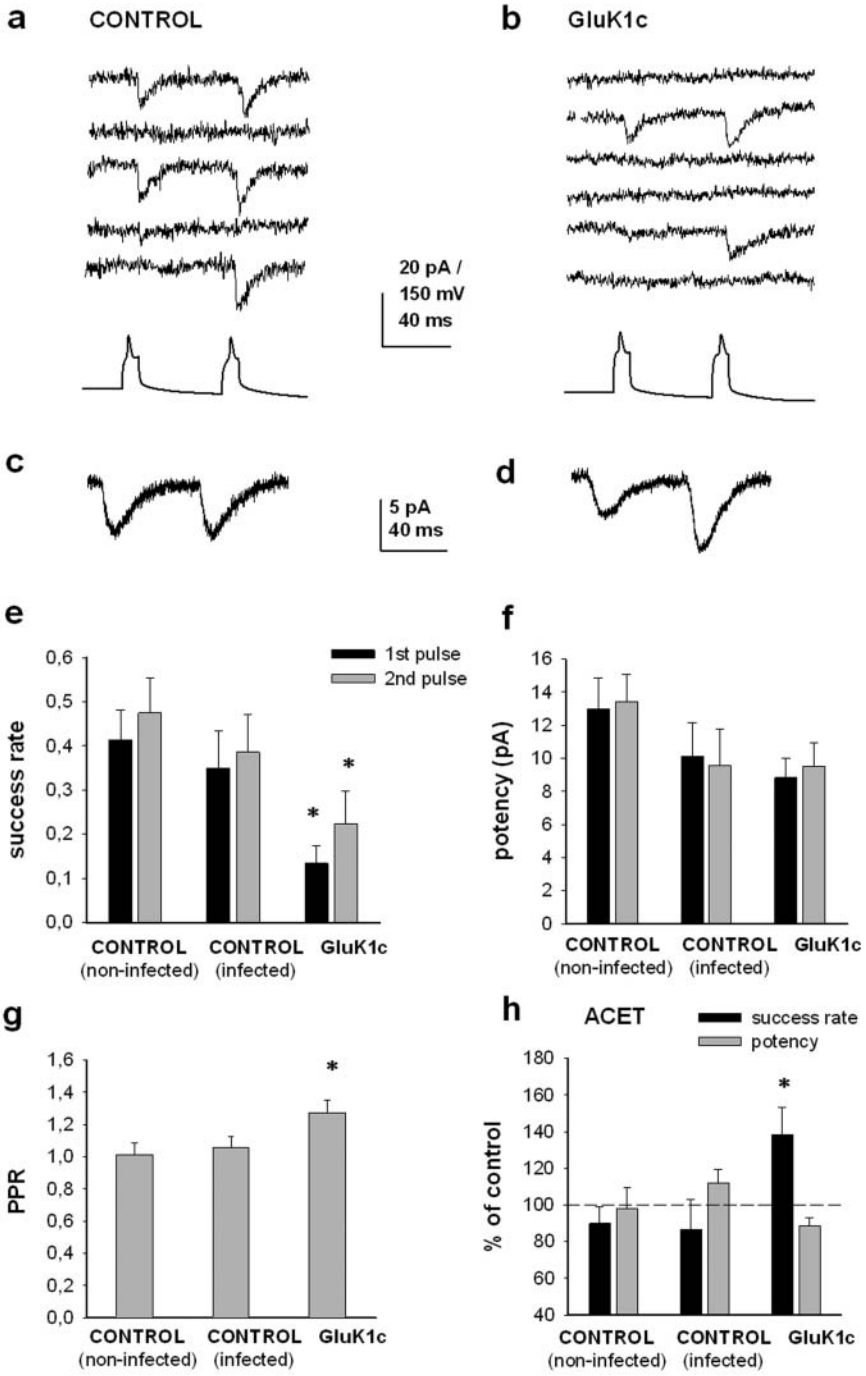

Figure 6 | Presynaptic expression of GluK1c inhibits glutamate release. (a,b) Example traces of whole cell recordings in CA3 pyramidal neuron pairs in organotypic slices. Five superimposed traces illustrate postsynaptic responses, recorded under voltage clamp under control conditions, and evoked by action-potential-inducing depolarization of the presynaptic neuron (bottom trace), that has been infected with a control virus (GluK1b_EGFP) (a) or GluK1c_EGFP (b). (c,d) Average of 20 consecutive traces, recorded in response to stimulation of control (c) and GluK1c (d) infected neurons. (e) Pooled data on the success rate of EPSCs in response to first and second depolarizing presynaptic pulse at control neuron pairs (non-infected, n=16; infected with control virus, n=13), as well as in pairs where GluK1c_EGFP is expressed presynaptically (n=12). (f) Analysis of the EPSC potency and paired pulse ratio (g) from the same data. (h) Normalized data on the effect of ACET (100 nM) on the success rate and potency of EPSCs, at control neuron pairs (non-infected n=5; infected n=4), as well as in pairs where GluK1c_EGFP is expressed presynaptically (n=4). All the error bars depict s.e.m. * $p<0.05$ with ANOVA.

GluK4/5. Upon formation of dendritic contact, axonal GluK1c was clearly detected at the dendritic contact sites, where it prominently co-localized with GluK4 and also (but apparently to lesser extent) with GluK5. These data fully support the idea that heteromeric KARs containing GluK1c and GluK4/5 subunits are presynaptically localized at immature synapses.

KARs have been implicated in physiological regulation of transmitter release in a variety of synapses, either via an ionotropic action facilitating presynaptic calcium dynamics and consequently, transmitter release, or via a G-protein dependent metabotropic mechanism that typically inhibits release (reviewed in 3). However, the molecular identity of presynaptic KARs and in

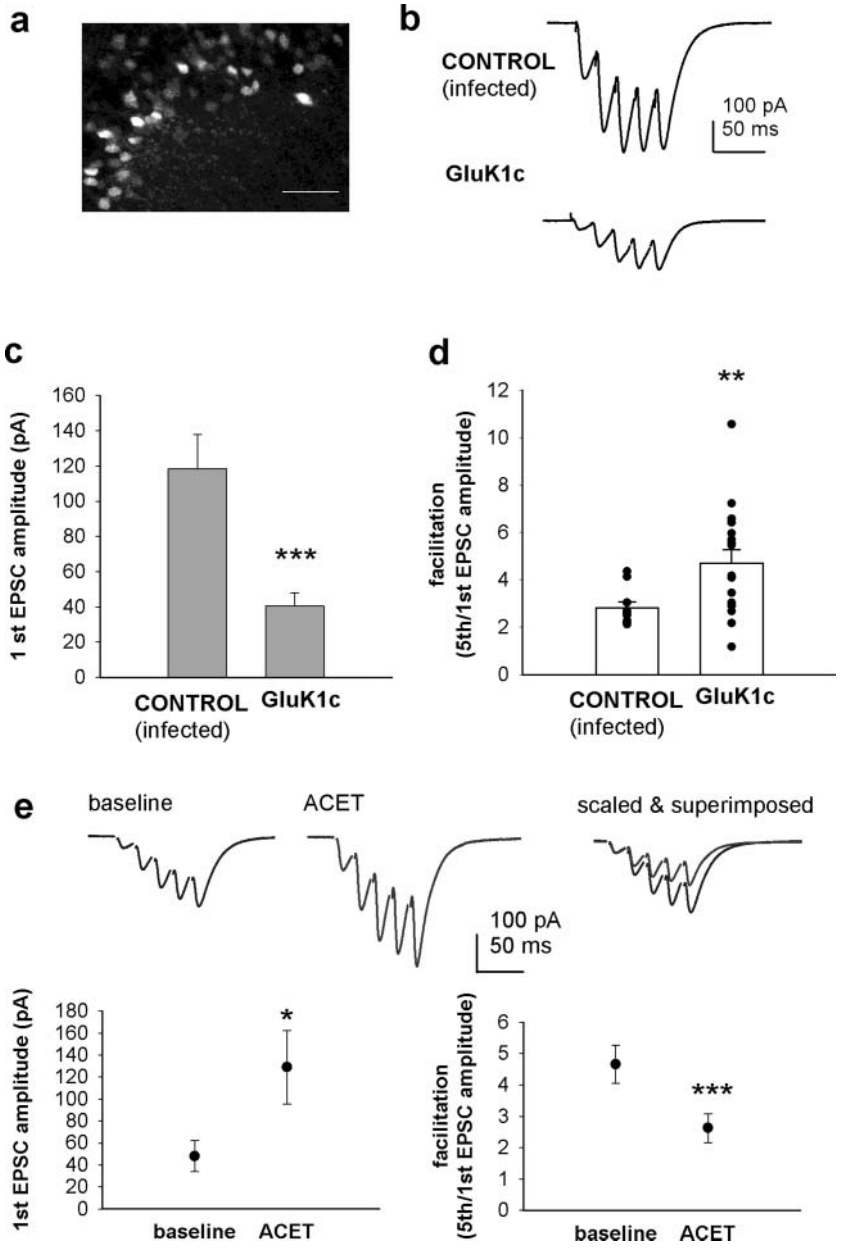

Figure 7 | The immature type KAR activity at CA3-CA1 synapses is mimicked by lentiviral expression of GluK1c in area CA3 at P14–P15.
(a) Fluorescence signal in the CA3 pyramidal area at P14, following local stereotaxic infection with EGFP- containing lentivirus at P1. Scale bar: 50 μm. (b) Example traces of EPSCs, recorded from CA1 pyramidal neurons in response to 5 pulse 50 Hz afferent stimulation in slices (P15) expressing EGFP (= control) or GluK1c_EGFP in area CA3. (c) Pooled data on the amplitude of the first EPSC in the train in slices (P14–P15) infected with a control virus (n=14) or GluK1c_EGFP (n=17) in area CA3. (d) Analysis of the facilitation ratio (amplitude of 5th/1st EPSC in the 50 Hz train) from the same data as in c. (e) The effect of ACET (100 nM) on EPSCs, evoked by 5 pulse 50 Hz stimulation in slices expressing GluK1c_EGFP in area CA3. Example traces of the synaptic response in control conditions and in the presence of ACET. Scaled and superimposed traces illustrate reduced facilitation in ACET. Pooled data (n=5) on the effect of ACET on the amplitude of the 1st EPSC and on facilitation ratio.

particular, the role of GluK1 subunit has been under debate, since pharmacological and genetic studies have given apparently contrasting results (e.g. [28,35]). Our recordings of cell pairs expressing GluK1c presynaptically provide compelling functional evidence for its involvement in the regulation of glutamate release. With this experimental approach, the spatially restricted expression of the gene construct as well as the cell-specific stimulation reduces the potential compensatory or indirect effects due to altered network behavior. Overexpression of the GluK1c in the presynaptic neuron lead to a robust reduction in the success rate of EPSCs, accompanied with an increase in paired pulse facilitation; both indicators of reduced probability of glutamate release. Interestingly, these effects were only partially reversed by application of the GluK1 selective antagonist ACET, suggesting that presynaptic GluK1c expression may cause also lasting changes in the functional connectivity[6].

The clear effect of the presynaptic GluK1c on transmission *in vitro* encouraged us to test whether the developmental KAR function can be recapitulated by expressing GluK1c in CA3 pyramidal neurons at two-three week old animals, where its endogenous expression is already downregulated. CA3 pyramidal neurons at juvenile and adult hippocampus express high levels of GluK4 mRNA[18,23], putatively

involved in axonal targeting and immature-type GluK1 function. Indeed, upon expression of GluK1c but not EGFP, an ACET-sensitive synaptic facilitation was detected in the CA3-CA1 synapses, similar to that seen during early postnatal development[5]. Thus, the expression of GluK1c is sufficient to mimic the immature – type KAR activity in a physiological tissue environment.

In conclusion, both the mRNA expression profile and the observed presynaptic effects of the GluK1c splice variant support its central role in mediating tonic inhibition of glutamate release in the immature hippocampal circuitry. This mechanism is involved in regulation of the endogenous network activity[9] as well as development of glutamatergic synaptic connectivity in the neonate hippocampus[5,6], directly defining the physiological significance of the developmentally restricted expression of the GluK1c and calling for detailed understanding of the signaling mechanisms specific for this splice variant.

Methods

Double *in situ* hybridization. Brains were taken from Wistar rats at postnatal days (P)3 and P15. The tissue was fixed in 4% paraformaldehyde (PFA), parafinated, and cut at 7 μm sections. The protocol for *in situ* hybridization was carried out essentially as described in ref.[36]. Oligodeoxyribonucleotide probes complementary to rat brain cDNAs are listed in the Supplementary Figure 1A. The fragments were cloned into a pGEM-T vector (Promega, Madison, WI). Clones were linearized by restriction digest and used as templates to generate sense and antisense S^{35}-labeled or Digoxigenin(dig) -labeled riboprobes. All probes were tested to ensure specific staining with anti-sense probe and that there was no nonspecific signal with the sense mRNA (Supplementary Figure 1b). In addition, the cross – reactivity between the probes designed to differentiate GluK1 b and –c splice variants was controlled using dot – blot assay (Supplementary Figure 1c).

Digital images were taken from stained sections using brightfield and darkfield optics to visualize dig and radioactive labeling, respectively. The colors in the dark field image were inverted and the image was superimposed with the corresponding brightfield figure. Brightness and contrast were adjusted digitally using Adobe Photoshop software to optimize signal to noise ratio. Calculations were made from the photomicrographs from at least four rectangular regions (150 μm×750 μm) positioned perpendicularly across the principal cell layer in areas CA1, CA3 and in the dentate gyrus. From each region, all cells positive for the radioactive stain (GluK1, GluK1b or GluK1c) were counted after which it was determined how many of these were double positive, i.e. labeled with dig (CaMKII-β, GluK4 or GluK5). The quantified data depicts the percentage of double positive cells of the cells detected by radioactive labeling. The percentage values were obtained by analyzing approximately 50 cells for each group (n values between 36–120; the low n values correspond to groups where the KAR expression level was very low).

RT- PCR. RNA was extracted from hippocampi of P3/P15 rats using RNeasy Mini Kit (Qiagen). cDNA was synthetized from 1 μg of total RNA with oligo-dT primers using RETROscript® (Ambion) reverse transcription (RT) kit. PCR on the RT products was performed in two rounds using common forward primers and GluK1 splice variant-specific reverse primers as indicated in the Table 1. The amplification products were separated on 2% agarose gel and stained with EtBr.

Generation of expression plasmids and lentiviral particles. Plasmids encoding epitope – tagged kainate-receptor subunits were constructed using a modified expression vector which contains a backbone of pEGFP-C1 (Clontech) and EGFP/Flag/6*Myc-epitope linked by multiple cloning sites (MCS) at both ends (dMCS). The cDNA of the various KAR subunits were generated by PCR from rat brain cDNA library, or from GluR5-2a/pRK7 (gift from A. Nishimune and J. Henley, University of Bristol, UK), and subcloned into the dMCS-vector in two steps; first the predicted signal sequence was inserted before the epitope into MCS I and then the rest of the sequence was cloned into MCS II. KA2-myc/pcDNA3 was kindly provided by F. Coussen and C. Mulle (University of Bordeaux, France). The epitope tagged constructs were subcloned into lentiviral transfer vector under synapsin or CMV promoter (pLen-Syn1/CMV; modified from pWPT-GFP, that was kindly provided by Didier Trono (Lausanne, Switzerland)). For electrophysiology experiments, 6*myc-tagged-GluK1b/c was cloned into pLen-vector containing two separate synapsin1 promoters, first driving the expression of GluK1 and the second the expression of EGFP. All constructs were verified by restriction mapping and by sequencing of PCR-amplified regions. The appropriate size of the encoded recombinant proteins was confirmed by western blot of transfected HEK293t cells.

For production of lentiviral particles, HEK293t cells were seeded at the density of 3×10^6 on 10 cm^2 plates and transfected with Fugene6 (Roche Applied Science) on the following day using 0.75 μg envelope-coding plasmid pMD.G, 2.25 μg packaging plasmid psPAX2 and 3 μg of transfer vector (derivate of the original pHR' backbone). Medium containing the viral particles was harvested 48 hours post-transfection, cleared of debris by low-speed-centrifugation and concentrated immediately by ultra-centrifugation (50 000 g, 2 hours at +4°C) or with PEG-*it*™ virus precipitation solution (System Biosciences). Pellets were suspended in DMEM or PBS in 1/100-1/200 of the original volume. The titers of the lentiviral stocks were determined with ELISA assay (Aalto Bioreagents) and were typically $1\times10^7-1\times10^8$ transducing units/ml.

Neuronal cultures and lentiviral infections. Hippocampi were dissected from 17/18-d-old rat embryos, treated with papain (500 μg/ml) and mechanically triturated to produce a single-cell suspension. Cells were seeded at the density of 40,000 cells/cm^2 on poly-L-ornithine (5 μg/ml, Sigma-Aldrich) + laminin (1.5 μg/cm^2, Sigma-Aldrich) -coated coverslips in Neurobasal medium with 2% B27 supplement, 0.5 mM L-glutamine, and 1x penicillin-streptomycin (all from Invitrogen). For compartmentalized cultures, the neurons were plated on microfluidic culture chambers that were mounted on poly-L-lysine (0.01%, Sigma) coated coverslips (24 mm×24 mm)[25,26]. Neuron cultures were infected with lentiviruses at 7–8 DIV (dispersed cultures) or 3 DIV (microfluidic cultures) by adding 1–3 μl of concentrated lentiviruses for 40,000 cells, so, that the transduction efficiency reached 70–100 %. Transduced neurons were analyzed at DIV 13–15.

Immunostaining of cultured neurons. For immunostainings, cells were washed with phosphate-buffered saline (PBS, pH 7.4) and fixed with 4% PFA in PBS for 15–20 minutes at room-temperature (RT). In experiments with compartmentalized cultures, coverslips containing fixed cells were detached from the microfluidic chamber. Fixed cells were either permeabilized with 0.25% Triton-X and blocked with 5% milk powder in PBS, or treated directly with blocking buffer containing 5% goat serum, 1% BSA, 0.1% gelatin, 0.1% Triton X-100, 0.05% Tween-20 in PBS. Primary antibodies (mouse anti-flag, 1 : 1500, Sigma-Aldrich; chicken anti-MAP2, 1 : 8000, Synaptic Systems and rabbit anti-Myc, 1 : 1500, Millipore) were added in blocking solution and cells were incubated over-night with shaking at +4°C. Cells were then washed several times with PBS before incubation with secondary antibodies (AlexaFluor 568 goat anti-mouse, AlexaFluor 488 goat anti-chicken, AlexaFluor 568 goat anti-chicken; AlexaFluor 488 goat anti-rabbit; AlexaFluor 405 goat anti-mouse; 1 : 500 dilution, Molecular Probes) for 1.5–2 hours RT. After washing the coverslips were mounted using FluorSave™ (Calbiochem) or ProlongGold Antifade (Iinvitrogen) reagent.

Immunostained samples of dispersed cultures were analysed with confocal microscope (Zeiss LSM 5 Pascal with Axioplan 2 microscope, using a C-Apochromat 40×, N.A 1.2 water objective). Images were taken at 1 μm interval, stacked and analyzed using Zeiss LSM Image Browser and Adobe photoshop software. Neurons from each image were grouped according to GluK1 localization: neurons in which GluK1 was localized strictly to soma (= restricted to soma-group) and neurons in which GluK1 was also detected in distal dendrites (>50 μm from the soma; distal dendrites-group). Axonal localization was defined as GluK1 positive but MAP2 (dendritic marker) negative processes. At least 150 neurons for each construct were analyzed. The quantified data depicts the percentage of cells in each group of all counted cells.

The images of microfluidic cultures were taken with MP Leica TCS SP5 confocal microscope, using HPX PL APO 63x 1.30 objective. Axonal processes, negative for MAP2 staining, 350–550 μm from the tunnel opening were used for quantification. Fluorescent images were taken at 0.5 to 0.75 μm interval, stacked and analyzed with Adobe Photoshop software. Bright field images were taken in parallel to determine total number of axons. On an average, 115 axons per condition were analyzed. The quantified data represents percentage of axons expressing KAR subunits with respect to total number of axons in mid part of tunnel in the same image frame. All the statistics have been calculated from the raw data.

Table 1 | Primers used for RT-PCR

First PCR	GluK1 forward1	TAAAAACAGTGACGAGGGGATCCA
	GluK1a reverse1	AGGGTTATCAAGGCATACGACAC
	GluK1bc reverse1	GGTGACAAGTAAGGATACTTGTG
Second PCR	Common forward primer2	CGATTGCCATTCTTCAACTGCAAG
	GluK1a reverse2	CAAGGCATACGACACTTCAGTA
	GluK1b reverse2	CATTGAAAGAGAGACACTGCTC
	GluK1c reverse2	GAAAGAGAGACACTTCTCTACACC
Control	GAPDH forward	CAACGACCCCTTCATTGACC
	GAPDH reverse	AGTGATGGCATGGACTGTGG

Dual recordings in hippocampal slice cultures. Organotypic cultures were prepared from postnatal day 7–8 (P7-8) Wistar rats as described previously[6]. Targeted lentiviral infections were done on the day after plating (DIV1), by injecting 1–2 µl of the lentiviral suspension to the CA3 area using a micromanipulator and Narishige IM-31 microinjector. For electrophysiological recordings, the cultures (9–11 DIV) were placed in a submerged recording chamber (RT) mounted on Olympus BX51 fluorescence microscope, and constantly superfused with an extracellular solution containing (mM): 124 NaCl, 3 KCl, 1.25 NaH_2PO_4, 1 $MgSO_4$, 26 $NaHCO_3$, 15 D-glucose, 2 $CaCl_2$ and 20 sucrose (320 mOsm; bubbled with 5% CO_2–95% O_2). Patch electrodes (3–5 MΩ) contained the following (mM): 140 K-gluconate, 10 Hepes, 2 KCl, 0.1 EGTA, 4 Mg-ATP, 0.5 Na-GTP and 20 sucrose (300 mOsm, pH 7.2). Infected neurons were identified based on EGFP fluorescence. Simultaneous whole-cell recordings were obtained from a fluorescent and non-fluorescent pyramidal neuron in CA3 area using Multiclamp 700A amplifier (Molecular Devices, USA). Brief depolarizing steps (10 ms, 500–800 pA) at 10 s intervals were given under current clamp to evoke action potentials in the fluorescent neuron while recording the activity of the non-fluorescent neuron under voltage-clamp (−70 mV). An inward current with amplitude at least three times the average noise level and with invariable delay less than 10 ms was considered as successful EPSC in the postsynaptic cell. Cell pairs with no detectable responses to 50 trials were rejected from the analysis. For calculation of the success rate and paired pulse facilitation ratio (with 50 ms inter-pulse interval), 50 successive sweeps were collected, after which ACET (100 nM) was applied extracellularly. Potency was calculated as the average amplitude of successful EPSCs.

In vivo infections and electrophysiology. Lentiviral particles were injected to the area CA3 of 0–2 day old rat pups under isoflurane anaesthesia. The animals were placed onto stereotaxic frame, the skull was exposed and a small hole was done using dental drill. 0.5 µl of lentiviral suspension was injected into CA3 region of hippocampus. The stereotaxic coordinates for CA3 were recalculated in the respect to bregma – lambda distance and varied in the following range: AP 1.8–2.2, ML 2.8–3.2, DV 2.8–3.0. The wound was treated with bacibact (Orion Pharma, Finland), sutured and the pup was left to recover with the dam. At P14–P15, acute hippocampal slices were made using standard methods (e.g. 5). Slices with clear fluorescence in area CA3 but not in CA1 were placed in a submerged recording chamber and perfused with extracellular solution containing (mM): NaCl, 124; KCl, 3; NaH_2PO_4, 1.25; $MgSO_4$, 1; $NaHCO_3$, 26; D-glucose, 10–15; $CaCl_2$, 2 ; 5% CO_2 / 95% O_2, RT. Whole cell voltage clamp recordings were made from CA1 pyramidal cells, with patch electrodes (2–5 MΩ) filled with a solution containing (in mM) $CsMeSO_4$, 130; HEPES, 10; EGTA, 0.5; Mg-ATP, 4; Na-GTP, 0.3; QX-314, 5; NaCl, 8; 285 mOsm, pH 7.2. AMPA-R mediated EPSCs were evoked by stimulation of Schaffer collateral-commissural fibres with a bipolar electrode, and recorded in the presence of antagonists of GABAA and NMDA receptors (picrotoxin (PiTX) [100 µM] and L689250 [5 µM], respectively). Baseline stimulation frequency was 1/20 sec. For train stimulation, 5 pulses were given at 50 Hz at 30 s intervals, and at least 10 trials were averaged for analysis. pClamp software was used for all data collection and analysis.

1. Collingridge, G. L., Olsen, R. W., Peters, J. & Spedding, M. A nomenclature for ligand-gated ion channels. *Neuropharmacology* **56**, 2–5 (2009).
2. Lerma, J. Roles and rules of kainate receptors in synaptic transmission. *Nat Rev Neurosci* **4**, 481 (2003).
3. Pinheiro, P. S. & Mulle, C. Presynaptic glutamate receptors: physiological functions and mechanisms of action. *Nat Rev Neurosci.* **9**, 423–36 (2008).
4. Contractor, A., Mulle, C. & Swanson, G. T. Kainate receptors coming of age: milestones of two decades of research. *Trends Neurosci.* **34**, 154–63 (2011).
5. Lauri, S. E., Vesikansa, A., Segerstråle, M., Collingridge, G. L., Isaac, J. T. R. & Taira, T. Functional maturation of CA1 synapses involves activity-dependent loss of tonic kainate receptor-mediated inhibition of glutamate release. *Neuron* **50**, 415–29 (2006).
6. Vesikansa, A., Sallert, M., Taira, T. & Lauri, S. E. Activation of kainate receptors controls density of functional glutamatergic synapses in the area CA1 of hippocampus. *J Physiol* **583**, 145–57 (2007).
7. Sallert, M., Malkki, H., Segerstråle, M., Taira, T. & Lauri, S. E. Effects of the kainate receptor agonist ATPA on glutamatergic synaptic transmission and plasticity during early postnatal development. *Neuropharmacology* **52**, 1354–65 (2007).
8. Sallert, M. *et al.* Brain-Derived Neurotrophic Factor Controls Activity-Dependent Maturation of CA1Synapses by Downregulating Tonic Activation of Presynaptic Kainate Receptors. *J. Neurosci.* **29**, 11294-11303 (2009).
9. Lauri, S. E. *et al.* Endogenous activation of kainate receptors regulates glutamate release and network activity ih the developing hippocampus. *J Neurosci* **25**, 4473 (2005).
10. Jane, D. E., Lodge, D. & Collingridge, G. L. Kainate receptors: pharmacology, function and therapeutic potential. *Neuropharmacology.* **56**, 90–113 (2009).
11. Jaskolski, F., Coussen, F., Nagarajan, N., Normand, E., Rosenmund, C. & Mulle, C. Subunit composition and alternative splicing regulate membrane delivery of kainate receptors. *J Neurosci.* **24**, 2506–15 (2004).
12. Hirbec, H. *et al.* Rapid and differential regulation of AMPA and kainate receptors at hippocampal mossy fibre synapses by PICK1 and GRIP. *Neuron* **37**(4), 625–38 (2003).
13. Werner, P., Voigt, M., Keinänen, K., Wisden, W. & Seeburg, P. H. Cloning of a putative high-affinity kainate receptor expressed predominantly in hippocampal CA3 cells. *Nature* **351**, 742–4 (1991).
14. Herb, A., Burnashev, N., Werner, P., Sakmann, B., Wisden, W. & Herb, A., Burnashev, N., Werner, P., Sakmann, B., Wisden, W. & Seeburg, P. H. The KA-2 subunit of excitatory amino acid receptors shows widespread expression in brain and forms ion channels with distantly related subunits. *Neuron* **8**, 775–85 (1992).
15. Mott, D. D., Rojas, A., Fisher, J. L., Dingledine, R. J. & Benveniste, M. Subunit-specific desensitization of heteromeric kainate receptors. *J Physiol* **588.4**, 683–700 (2010).
16. Paternain, A. V., Herrera, M. T., Nieto, M. A. & Lerma, J. GluR5 and GluR6 kainate receptor subunits coexist in hippocampal neurons and coassemble to form functional receptors. *J Neurosci.* **20**, 196–205 (2000).
17. Bureau, I., Bischoff, S., Heinemann, S. F. & Mulle, C. Kainate receptor-mediated responses in the CA1 field of wild-type and GluR6-deficient mice. *J Neurosci.* **19**, 653–63 (1999).
18. Wisden, W. & Seeburg, P. H. A complex mosaic of high-affinity kainate receptors in rat brain. *J Neurosci.* **13**, 3582–98 (1993).
19. Bahn, S., Volk, B. & Wisden, W. Kainate receptor gene expression in the developing rat brain. *J Neurosci* **14**, 5525 (1994).
20. Ritter, L. M., Vazquez, D. M. & Meador-Woodruff, J. H. Ontogeny of ionotropic glutamate receptor subunit expression in the rat hippocampus. *Brain Res Dev Brain Res.* **139**, 227–36 (2002).
21. Burgin, K. E., Waxham, M. N., Rickling, S., Westgate, S. A., Mobley, W. C. & Kelly, P. T. In situ hybridization histochemistry of Ca2+/calmodulin-dependent protein kinase in developing rat brain. *J. Neurosci.* **10**, 1788–1798 (1990).
22. Bayer, K. U., Lohler, J., Schulman, H. & Harbers K. Developmental expression of the CaM kinase II isoforms: ubiquitous gamma- and delta-CaM kinase II are the early isoforms and most abundant in the developing nervous system. *Brain Res. Mol. Brain Res.* **70**, 147–154 (1999).
23. Kask, K., Jerecic, J., Zamanillo, D., Wilbertz, J., Sprengel, R. & Seeburg, P. H. Developmental profile of kainate receptor subunit KA1 revealed by Cre expression in YAC transgenic mice. *Brain Res* **876**, 55–61 (2000).
24. Kayadjanian, N., Lee, H. S., Piña-Crespo, J. & Heinemann, S. F. Localization of glutamate receptors to distal dendrites depends on subunit composition and the kinesin motor protein KIF17. *Mol Cell Neurosci* **34**, 219–30 (2007).
25. Taylor, A. M., Blurton-Jones, M., Rhee, S. W., Cribbs, D. H., Cotman, C. W. & Jeon, N. L. A microfluidic culture platform for CNS axonal injury, regeneration and transport. *Nat. Methods* **2**, 599–605 (2005).
26. Taylor, A. M., Dieterich, D. C., Ito, H. T., Kim, S. A. & Schuman, E. M. Microfluidic local perfusion chambers for the visualization and manipulation of synapses. *Neuron* **66**, 57–68 (2010).
27. Dargan, S. L. *et al.* ACET is a highly potent and specific kainate receptor antagonist: characterisation and effects on hippocampal mossy fibre function. *Neuropharmacology* **56**, 121–30 (2009).
28. Liu, X., Tilwalli, S., Ye, G., Lio, P. A., Pasternak, J. F. & Trommer, B. L. Morphologic and electrophysiologic maturation in developing dentate gyrus granule cells. *Brain Res.* **856**,202–212 (2000).
29. Lauri, S. E. *et al.* A critical role of a facilitatory kainate autoreceptor in mossy fibre LTP. *Neuron* **32**, 697–709 (2001).
30. Caiati, M. D., Caiati, M. D., Sivakumaran, S. & Cherubini, E. In the developing rat hippocampus, endogenous activation of presynaptic kainate receptors reduces GABA release from mossy fiber terminals. *J Neurosci.* **30**, 1750–9 (2010).
31. Maingret, F., Lauri, S. E., Taira, T. & Isaac, J. T. R. Profound regulation of neonatal CA1 rat hippocampal GABAergic transmission by functionally distinct kainate receptor populations. *J Physiol* **567**, 131–42 (2005)
32. Segerstråle, M. *et al.* High firing rate of neonate hippocampal interneurons is due to attenuation of afterhyperpolarizing potassium current by tonically active kainate receptors. *J Neurosci.* **30**, 6507–14 (2010).
33. Swanson, G. T. *et al.* Differential Activation of Individual Subunits in Heteromeric Kainate Receptors. *Neuron* **34**, 589–598 (2002).
34. Fernandes, H. B. *et al.* High-affinity kainate receptor subunits are necessary for ionotropic but not metabotropic signaling. *Neuron* **63**, 818–29 (2009).
35. Contractor, A., Swanson, G. T., Sailer, A., O'Gorman, S. & Heinemann, S. F. Identification of the kainate receptor subunits underlying modulation of excitatory synaptic transmission in the CA3 region of the hippocampus. *J Neurosci.* **20**, 8269–78 (2000).
36. Huberfeld, G. *et al.* Perturbed chloride homeostasis and GABAergic signaling in human temporal lobe epilepsy. *J Neurosci.* **27**, 9866–73 (2007).

Acknowledgements

We thank Marina Tibeikina and Miika Palviainen for excellent help in performing *in vivo* viral infections and *in situ* hybridizations, respectively. The work is supported by the Academy of Finland, the Sigrid Juselius foundation and the University of Helsinki research funds as well as the Helsinki Graduate School of Biotechnology and Molecular Biology (A.V., P.S.).

Author contributions

A.V., P.S. and S.E.L. conducted the majority of the experiments and performed analysis. A.V. and J.K-P. designed and produced the viral vectors. S.M. set up the *in vivo* injections. C.R., H.H., H.R. T.T. and S.E.L. contributed to the project design and infrastructure. A.V. and S.E.L. wrote the manuscript. All authors reviewed the manuscript.

Additional information

Supplementary information accompanies this paper at http://www.nature.com/scientificreports

Competing financial interests: The authors declare no competing financial interests.

How to cite this article: Vesikansa, A. *et al.* Expression of GluK1c underlies the developmental switch in presynaptic kainate receptor function. *Sci. Rep.* **2**, 310; DOI:10.1038/srep00310 (2012).